ChemComm

COMMUNICATION

View Article Online
View Journal

Cite this: DOI: 10.1039/c7cc03477f

Received 4th May 2017,
Accepted 20th May 2017

DOI: 10.1039/c7cc03477f

rsc.li/chemcomm

Rapid and efficient tetrazine-induced drug release from highly stable benzonorbornadiene derivatives†

Minghao Xu, Julian Tu and Raphael M. Franzini *

A novel class of bioorthogonal release reactions based on benzonorbornadiene derivatives was developed. These carrier molecules are highly stable at physiological conditions, but react rapidly with 1,2,4,5-tetrazines, and near-quantitatively release cargo molecules such as drugs and optical reporters.

The advent of bioorthogonal reactions opened the unprecedented opportunity to perform chemistry in living organisms.[1] Biocompatible reaction development has focused primarily on transformations that link two molecules, and bioorthogonal ligation reactions boast broad applicability in chemical biology, materials science, and to localize drugs and imaging agents at sites of disease.[2,3] In contrast, the discovery of bioorthogonal cleavage reactions that allow for the controlled release of payloads has only recently attracted substantial research interest.[4] Nevertheless, such reactions are valuable in a wide range of applications. Representative examples include biodetection probes,[5,6] DNA sequencing,[7] protein activity control,[8–10] and multiplexed cell imaging.[11] The use of dissociative *in vivo* chemistry to enable the spatiotemporally controlled release of drugs is particularly appealing because of the potential for clinical translation in cancer chemotherapy. For example, implantation of tetrazine (Tz)-modified biomaterials enabled the localized activation of doxorubicin prodrugs with superior therapeutic index relative to systemic drug administration.[12] Alternatively, bioorthogonal reactions could activate antibody-drug conjugates *in vivo*.[13] In this pretargeting strategy, an antibody modified with a drug *via* a chemically-cleavable linker accumulates at the desired site, and subsequent administration of a trigger molecule liberates the cytotoxic agent tissue specifically.[13]

The scarcity of bioorthogonal bond-cleavage reactions remains a key bottleneck for the advancement of reaction-based applications in chemical biology and smart therapeutics. Until recently, modified Staudinger reactions were the only available bioorthogonal release reactions.[5,14–16] The development of the inverse-electron demand Diels–Alder (IEDDA) pyridazine elimination reaction of carbamate-modified *trans*-cyclooctenes (TCO) and Tz was a breakthrough with this regard.[17,18] This reaction is significantly faster than the Staudinger reaction, obviates the use of metabolically unstable phosphines, and is widely used in chemical biology.[7,10,12,13] Further examples of bioorthogonal cleavage reactions are the strain-promoted 1,3-dipolar cycloaddition of TCO and *p*-azidobenzylcarbamates,[19] and the Tz-mediated removal of vinyl ethers.[6,20,21] However, reactions need to meet several strict requirements for *in vivo* use, including rapid reaction rate, near-quantitative payload release, lack of toxicity, and prolonged serum stability. Current reactions meet these conditions only partially and further development will be necessary to achieve the full potential of *in vivo* drug activation.

Here we describe benzonorbornadiene (BNBD) derivatives as stable carrier molecules that rapidly react with Tz to near-quantitatively release a cargo molecule (*e.g.* cytotoxic agent, optical reporter). Our design harnesses the intrinsic lability of isobenzofurans/isoindoles to liberate a molecule of interest. These self-immolative heterocycles are readily accessible by the reaction of BNBDs and Tz.[22] Devaraj *et al.* have used this transformation for nucleic acid sensing but their design lacked the capability of releasing a molecule.[23] In particular, the proposed release molecules consist of 7-aza/oxa-BNBDs with carbamate leaving groups attached *via* a methylene linker to the bridgehead carbon (Scheme 1). The reaction of 7-aza/oxa-BNBDs with Tz is anticipated to generate an intermediate (**I1**), which rapidly eliminates N_2, followed by a retro Diels–Alder cycloreversion, generating isoindoles/isobenzofurans (**I3**).[22] These heterocycles in turn eliminate the carbamate to liberate the free amine (Scheme 1a). In contrast to the reaction intermediates, the BNBD precursors are expected to be highly stable.

To test the outlined bioorthogonal release reaction, we synthesized three BNBD derivatives with oxygen (**1**), acetamide (**2**), and Boc-protected nitrogen (**3**) at position 7 of the BNBD bicycle and a (*p*-nitrophenylcarbamoyl)methyl substituent at

Department of Medicinal Chemistry, College of Pharmacy, University of Utah, 30 S 2000 E, Salt Lake City, UT-84112, USA. E-mail: raphael.franzini@utah.edu

† Electronic supplementary information (ESI) available: Detailed experimental procedures, supporting figures, and tables. See DOI: 10.1039/c7cc03477f

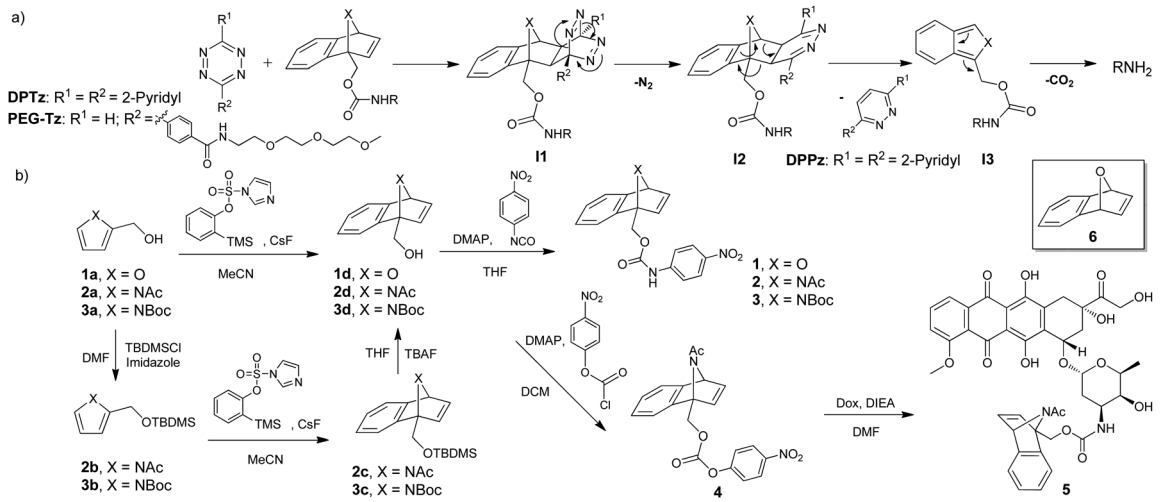

Scheme 1 7-aza/oxa-benzonorbornadiene (BNBD) derivatives as bioorthogonal drug release molecules. (a) Proposed mechanism of tetrazine-inducible cargo release. (b) Synthesis of 7-aza/oxa-BNBD derivatives **1–3** and doxorubicin prodrug **5**. Compound **6** is a control molecule used in kinetics experiments.

the bridgehead carbon (Scheme 1b). The different substituents in **1–3** were selected to test the influence of the heterocycle on reaction rate and cargo release. *p*-Nitroaniline (pNA) was used as the reporter for bond-cleavage because a bathochromic shift from λ_{max} = 317 nm to λ_{max} = 378 nm accompanies carbamate to aniline conversion. The synthesis of **1–3** (Scheme 1b) started from furfuryl alcohol (**1a**) and *N*-acetyl- or *N*-Boc-(2-hydroxymethyl)pyrroles (**2a**, **3a**). A [4+2] cycloaddition reaction of these heterocylces with benzyne afforded the bicyclic structures **1d–3d**. The pyrroles required TBDMS-protection of the hydroxymethyl group (**2b**, **3b**) for the benzyne reaction. Reaction of hydroxymethyl bicycles **1d–3d** with (4-nitrophenyl)isocyanate provided the desired release structures **1–3**. The straightforward synthesis of these molecules compares favorably to TCO-prodrugs that require tedious multi-step synthesis, including the separation of the axial from the equatorial stereoisomer.[13]

We first investigated whether the reaction of BNBD-derivatives with Tz released pNA (Fig. 1). Incubation of **1–3** with 3,6-di-(2-pyridyl)-1,2,4,5-tetrazine (DPTz) resulted in a distinct color change, which indicated complete DPTz consumption and efficient pNA release. **1–3** were completely stable under these conditions (data not shown). HPLC monitoring of the reaction (c(**1–3**) = 6 mM, c(DPTz) = 18 mM, T = 37 °C, DMSO/H_2O (9 : 1)) confirmed complete consumption of **1–3**, disappearance of DPTz, and formation of two new elution peaks that were identified as pNA and 3,6-di-(2-pyridyl)-1,2-pyridazine (DPPz) based on LC-MS (Fig. 1 and Fig. S2–S4, ESI†). The starting BNBD was the only perceptible peak with an absorbance maximum at λ_{max} = 317 nm and intermediates **I1–I3** or side-products with trapped pNA were undetectable. Isoindole/isobenzofuran decomposition products were visible in the HPLC traces at later measurements. These results demonstrated the rapid and high-yielding release of pNA.

We further measured the kinetics of the reaction of **1–3** and Tz. Photospectrometric analysis of DPTz disappearance (λ_{abs} = 525 nm) in the presence of excess BNBDs revealed pseudo-first order

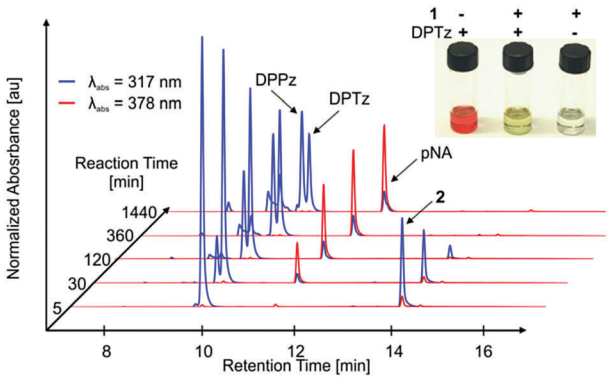

Fig. 1 Release of pNA from 7-aza/oxa-BNBDs. HPLC analysis of reaction **2** with DPTz (c(**1**) = c(DPTz) = 6 mM, 24 h, RT). Inset: Color change resulting from reaction of **1** and DPTz.

kinetics, and the concentration dependence of the rate constants agreed with a second-order rate law. In DMSO, the second order rate constants (k_2) were 0.015 M^{-1} s^{-1} for **1**, 0.010 M^{-1} s^{-1} for **2**, and 0.0044 M^{-1} s^{-1} for **3** (Table 1 and Fig. S1, ESI†). The differences in the rate constants reflect the increase in steric repulsion from **1** to **3** although electronic effects may also influence the rate.[24] Comparison of the kinetics of the reaction of DPTZ with **1** to that with 7-oxo-BNBD (**6**, Scheme 1b; k_2 = 0.176 M^{-1} s^{-1}) revealed that the carbamoyl-methyl substituent decreased the reaction rate ~12-fold. Presence of 10% H_2O accelerated the reaction 1.7 to 1.9-fold (Table 1). This result is consistent with reported rate-enhancing effects of H_2O on IEDDA reactions.[21,25] We prepared a water-soluble Tz (PEG–Tz; Scheme 1a) to test the solvent effect on the kinetics. Increasing the H_2O content further (DMSO/PBS, 3 : 2) accelerated the reaction rate of **2** (k_2 = 0.135 M^{-1} s^{-1}) and **1** (k_2 = 0.190 M^{-1} s^{-1}) with PEG–Tz. The reaction of **1** and **2** with Tz was significantly faster than the release reaction of TCO with aromatic azides (k_2 = 0.027 M^{-1} s^{-1}),[19] Tz-induced uncaging of vinyl ethers (k_2 = 0.00021 M^{-1} s^{-1}),[20,21] and dissociative Staudinger reactions (k_2 = ~0.001 M^{-1} s^{-1}).[1] Only the IDEEA

Table 1 Second-order rate constants (k_2) for reactions of **1–3** and tetrazines[a]

Pb	Tz	DMSO [M^{-1} s^{-1}]	90%DMSO/H_2O	60%DMSO/PBS
1	DPTz	0.015 ± 0.008	0.028 ± 0.0003	—
2	DPTz	0.010 ± 0.0004	0.017 ± 0.002	—
3	DPTz	0.0044 ± 0.0009	0.0084 ± 0.0016	—
6	DPTz	0.176 ± 0.004	—	—
1	PEG–Tz	—	0.058 ± 0.0003	0.190 ± 0.029
2	PEG–Tz	—	0.020 ± 0.0007	0.135 ± 0.010

[a] The reactions were monitored by time-dependent absorbance measurements at λ_{abs} = 525 nm and T = 37 °C.

pyridazine release reaction surpasses this rate.[17,18] For several bioorthogonal cycloaddition reactions, simple structural changes were sufficient to enhance reaction rates by orders of magnitude and efforts are ongoing to further accelerate the reaction of BNBDs with Tz for *in vivo* applications.

To quantify pNA release and to analyze the mechanism of the reaction of **1–3** and DPTz, we monitored the transformation by ^{1}H NMR (Fig. 2 and Fig. S5–S8, ESI†). Solutions of **1–3** and DPTz in DMSO-d_6 or DMSO-d_6/D_2O (9 : 1) were incubated at 37 °C and ^{1}H NMR spectra were recorded periodically over 24 h. At these conditions, DPTz near-completely consumed BNBD derivatives within 2 h in agreement with results from HPLC analysis (Fig. 1) and kinetics measurements (Table 1). NMR peaks corresponding to pNA emerged concomitant with disappearance of **1–3**, indicating rapid and efficient cargo liberation (Fig. 2). The measured pNA release from **1** and **2** in DMSO-d_6/D_2O at 6 h and 24 h was in the range of 80–90%; release of pNA from **3** was less efficient (Fig. 2b). Experiments with PEG–Tz provided similar results (Fig. S9, ESI†).

^{1}H NMR integration analysis revealed that in case of **1**, pNA formation was delayed relative to BNBD consumption (Fig. S5, ESI†). A singlet peak at 5.59 ppm was present in early ^{1}H NMR spectra but disappeared with prolonged incubation. Integration of this peak accounted for the difference between consumed **1** and released pNA, and we postulate that it corresponds to the heterocyclic intermediate **I3** (Fig. S10, ESI†). In contrast, consumption of **2** and DPPz formation occurred in parallel with pNA generation, and ^{1}H NMR peaks consistent with the structure of **I3** were absent (Fig. 2a and c). Peaks corresponding to the 1,4-isomer of intermediate **I2** were not visible but may be formed in quantities below the experimental detection limit or as transient species. These results demonstrate that isoindoles **I3** release amines rapidly and near-quantitatively.

Given the Tz-induced liberation of pNA, we evaluated the potential of BNBDs in a prodrug activation strategy. A 7-acetamide–BNBD doxorubicin prodrug (**5**) was synthesized *via* **2d** (Scheme 1b). HPLC analysis of the reaction between **5** and PEG–Tz (DMSO, T = 37 °C, c(**5**) = 0.2 mM, c(PEG–Tz) = 1.6 mM) showed rapid and complete doxorubicin release (Fig. S12, ESI†). We further tested Tz-triggered drug release in cell viability assays. Addition of doxorubicin-prodrug **5** followed by PEG–Tz caused dose-dependent cytotoxicity in A549 pulmonary adenocarcinoma cells (EC_{50}(**5** + 200 μM PEG–Tz) = 96 nM), rivaling that of doxorubicin (EC_{50}(Dox) = 88 nM, Table 2). Conversely, the prodrug **5** alone was essentially non-toxic in the tested concentration range (EC_{50}(**5**) > 10 μM; Table 2) and only at the highest concentrations was mild cytotoxicity observed. The combination of high BNBD stability and facile drug release will be essential for achieving a high therapeutic index in targeted drug delivery approaches. The cytotoxic effect of **5** was nearly preserved at 100 μM PEG–Tz (EC_{50}(**5** + 100 μM PEG–Tz) = 99 nM) but gradually decreased when lowering the PEG–Tz concentration further (Table 2). At the lowest tested concentration c(PEG–Tz) = 25 μM, the EC_{50} was 0.521 μM, which corresponds to 10–20%

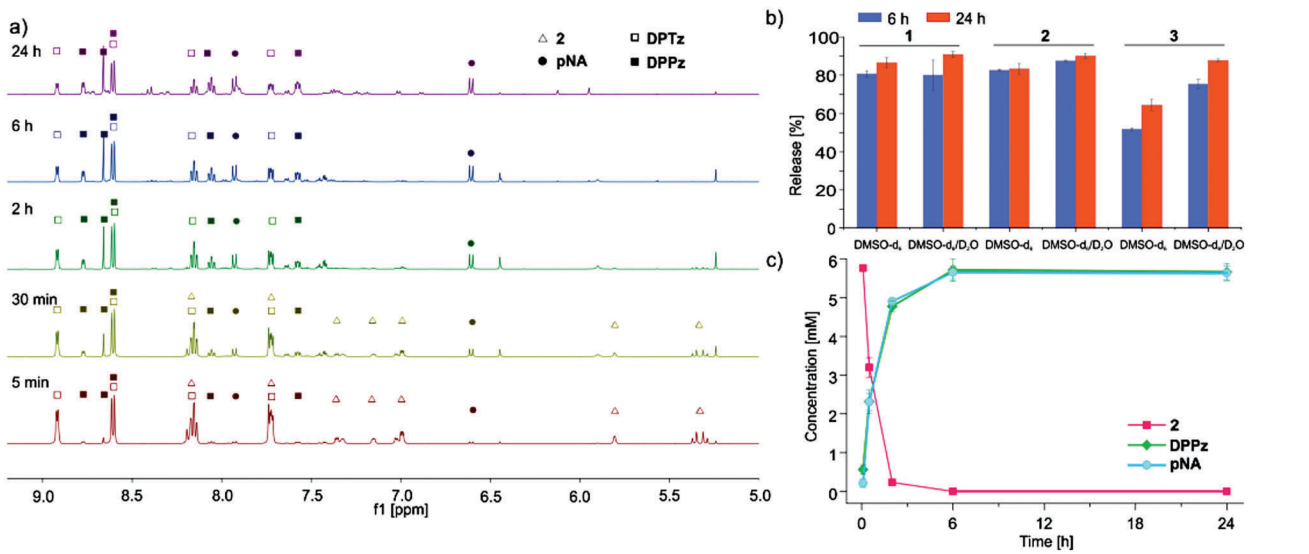

Fig. 2 ^{1}H NMR analysis of bioorthogonal bond cleavage reaction of BNBDs and Tz. (a) Time-dependent pNA release from **2**. (b) Quantification of the release of *p*-nitroaniline (pNA) from 7-aza/oxa-BNBD **1–3**. (c) Concentrations of starting material (**2**) and reaction product (DPPz, pNA) as a function of time. Fig. 1. Release of pNA from 7-aza/oxa-BNBDs. HPLC analysis of reaction **2** with DPTz (c(**2**) = c(DPTz) = 6 mM, 24 h, RT). Inset: Color change resulting from reaction of **1** and DPTz.

Table 2 Cytotoxicity of activated prodrug **5**, 72 h incubation at 37 °C[a]

Compounds	EC_{50} (μM) in A549 cells
Doxorubicin	0.088 ± 0.031
5 + PEG–Tz (200 μM)	0.096 ± 0.022
5 + PEG–Tz (100 μM)	0.099 ± 0.029
5 + PEG–Tz (50 μM)	0.128 ± 0.017
5 + PEG–Tz (25 μM)	0.521 ± 0.192
5	>10
2 + PEG–Tz (100 μM)	>10
PEG–Tz	>200

[a] The proliferation assay was performed in at least triplicate and EC_{50} values were derived from the normalized cell growth.

released doxorubicin and the combination with **5** was >20-fold more toxic than the prodrug alone, emphasizing the high stability of **5** (Table 2). Tz molecules are rather non-toxic,[13] and mice in a previous animal study showed no adverse reactions to repeated intravenous injection of doses as high as 1250 μmol kg^{-1}.[8] Indeed, control samples with PEG–Tz showed no cytotoxicity even at the highest concentration tested (200 μM). Also, combination of PEG–Tz and **2** resulted in minimal toxicity in the tested concentration range (Fig. S15, ESI†) demonstrating that cells tolerate isoindole decomposition products well.

We directly tested the stability of **5** in DMSO/PBS and human serum. **5** was inert for 48 h, and no free doxorubicin or doxorubicin-containing side products were observed by HPLC (Fig. S11 and S13, ESI†). The quantity of **5** decreased with longer incubation times but no free doxorubicin was detectable (Fig. S13, ESI†). In light of the instability of doxorubicin in serum, we reasoned that decomposition of doxorubicin rather than the BNBD linker caused the observed effect. To test this hypothesis, we measured the serum-stability of **2** and this BNBD was completely stable until the end of the analysis at one week and no traces of pNA were formed (Fig. S14, ESI†). Additionally, BNBD derivatives are expected to retain their reactivity in contrast to TCO-derived molecules that gradually deactivate by spontaneous *trans*/*cis* isomerization.[13,17]

In conclusion, we have developed a novel and promising bioorthogonal reaction for the traceless release of a molecular cargo. In our design, derivatives of BNBD react with Tz and liberate a drug or optical reporter *via* unprecedented hydrolysis-susceptible isoindole/isobenzofuran intermediates. The reaction exhibits favorable characteristics including quantitative as well as prompt payload release, rapid bimolecular reaction, low reagent toxicity, and exceptional probe stability at physiological conditions. The straightforward synthesis of the BNBD precursors is another advantage of the release design. This reaction boasts great promise for application in reaction-based prodrug strategies. Additionally, BNBDs may find widespread applications in chemical biology for example in detection probes and for enzyme activation.

We gratefully acknowledge financial support from the University of Utah, the Huntsman Cancer Institute, and the USTAR initiative. We thank the group of Dr S. Sharma (HCI) for help with cell experiments.

Notes and references

1 E. M. Sletten and C. R. Bertozzi, *Angew. Chem., Int. Ed. Engl.*, 2009, **48**, 6974–6998.
2 J. M. Mejia Oneto, M. Gupta, J. K. Leach, M. Lee and J. L. Sutcliffe, *Acta Biomater.*, 2014, **10**, 5099–5105.
3 R. Rossin, P. R. Verkerk, S. M. van den Bosch, R. C. Vulders, I. Verel, J. Lub and M. S. Robillard, *Angew. Chem., Int. Ed. Engl.*, 2010, **49**, 3375–3378.
4 J. Li and P. R. Chen, *Nat. Chem. Biol.*, 2016, **12**, 129–137.
5 R. M. Franzini and E. T. Kool, *J. Am. Chem. Soc.*, 2009, **131**, 16021–16023.
6 H. Wu, S. C. Alexander, S. Jin and N. K. Devaraj, *J. Am. Chem. Soc.*, 2016, **138**, 11429–11432.
7 D. R. Bentley, *et al.*, *Nature*, 2008, **456**, 53–59.
8 J. Li, S. Jia and P. R. Chen, *Nat. Chem. Biol.*, 2014, **10**, 1003–1005.
9 J. Luo, Q. Liu, K. Morihiro and A. Deiters, *Nat. Chem.*, 2016, **8**, 1027–1034.
10 G. Zhang, J. Li, R. Xie, X. Fan, Y. Liu, S. Zheng, Y. Ge and P. R. Chen, *ACS Cent. Sci.*, 2016, **2**, 325–331.
11 M. Mondal, R. Liao, L. Xiao, T. Eno and J. Guo, *Angew. Chem., Int. Ed. Engl.*, 2017, **56**, 2636–2639.
12 J. M. Mejia Oneto, I. Khan, L. Seebald and M. Royzen, *ACS Cent. Sci.*, 2016, **2**, 476–482.
13 R. Rossin, S. M. van Duijnhoven, W. Ten Hoeve, H. M. Janssen, L. H. Kleijn, F. J. Hoeben, R. M. Versteegen and M. S. Robillard, *Bioconjugate Chem.*, 2016, **27**, 1697–1706.
14 M. J. Hangauer and C. R. Bertozzi, *Angew. Chem., Int. Ed. Engl.*, 2008, **47**, 2394–2397.
15 R. van Brakel, R. C. Vulders, R. J. Bokdam, H. Grull and M. S. Robillard, *Bioconjugate Chem.*, 2008, **19**, 714–718.
16 K. Gorska, A. Manicardi, S. Barluenga and N. Winssinger, *Chem. Commun.*, 2011, **47**, 4364–4366.
17 R. M. Versteegen, R. Rossin, W. ten Hoeve, H. M. Janssen and M. S. Robillard, *Angew. Chem., Int. Ed. Engl.*, 2013, **52**, 14112–14116.
18 X. Fan, Y. Ge, F. Lin, Y. Yang, G. Zhang, W. S. Ngai, Z. Lin, S. Zheng, J. Wang, J. Zhao, J. Li and P. R. Chen, *Angew. Chem., Int. Ed. Engl.*, 2016, **55**, 14046–14050.
19 S. S. Matikonda, D. L. Orsi, V. Staudacher, I. A. Jenkins, F. Fiedler, J. Chen and A. B. Gamble, *Chem. Sci.*, 2015, **6**, 1212–1218.
20 K. Neumann, S. Jain, A. Gambardella, S. E. Walker, E. Valero, A. Lilienkampf and M. Bradley, *ChemBioChem*, 2017, **18**, 91–95.
21 E. Jimenez-Moreno, Z. Guo, B. L. Oliveira, I. S. Albuquerque, A. Kitowski, A. Guerreiro, O. Boutureira, T. Rodrigues, G. Jimenez-Oses and G. J. Bernardes, *Angew. Chem., Int. Ed. Engl.*, 2016, **56**, 243–247.
22 G. M. Priestley and R. N. Warrener, *Tetrahedron Lett.*, 1972, **13**, 4295–4298.
23 H. Wu, B. T. Cisneros, C. M. Cole and N. K. Devaraj, *J. Am. Chem. Soc.*, 2014, **136**, 17942–17945.
24 A. C. Knall, M. Hollauf and C. Slugovc, *Tetrahedron Lett.*, 2014, **55**, 4763–4766.
25 A. C. Knall, M. Hollauf, R. Saf and C. Slugovc, *Org. Biomol. Chem.*, 2016, **14**, 10576–10580.

